Cancer Research

MicroRNA Mediates DNA Demethylation Events Triggered by Retinoic Acid during Neuroblastoma Cell Differentiation

Sudipto Das[1,2], Niamh Foley[1,2], Kenneth Bryan[1,2], Karen M. Watters[1,2], Isabella Bray[1,2], Derek M. Murphy[1,2], Patrick G. Buckley[1,2], and Raymond L. Stallings[1,2]

Abstract

Neuroblastoma is an often fatal pediatric cancer arising from precursor cells of the sympathetic nervous system. 13-Cis retinoic acid is included in the treatment regimen for patients with high-risk disease, and a similar derivative, all-*trans*-retinoic acid (ATRA), causes neuroblastoma cell lines to undergo differentiation. The molecular signaling pathways involved with ATRA-induced differentiation are complex, and the role that DNA methylation changes might play are unknown. The purpose of this study was to evaluate the genome-wide effects of ATRA on DNA methylation using methylated DNA immunoprecipitation applied to microarrays representing all known promoter and CpG islands. Four hundred and two gene promoters became demethylated, whereas 88 were hypermethylated post-ATRA. mRNA expression microarrays revealed that 82 of the demethylated genes were overexpressed by >2-fold, whereas 13 of the hypermethylated genes were underexpressed. Gene ontology analysis indicated that demethylated and re-expressed genes were enriched for signal transduction pathways, including *NOS1*, which is required for neural cell differentiation. As a potential mechanism for the DNA methylation changes, we show the downregulation of methyltransferases, *DNMT1* and *DNMT3B*, along with the upregulation of endogenous microRNAs targeting them. Ectopic overexpression of miR-152, targeting *DNMT1*, also negatively affected cell invasiveness and anchorage-independent growth, contributing in part to the differentiated phenotype. We conclude that functionally important, miRNA-mediated DNA demethylation changes contribute to the process of ATRA-induced differentiation resulting in the activation of *NOS1*, a critical determinant of neural cell differentiation. Our findings illustrate the plasticity and dynamic nature of the epigenome during cancer cell differentiation. *Cancer Res; 70(20); 7874–81. ©2010 AACR.*

Introduction

Neuroblastoma is an often fatal cancer of childhood arising from precursor cells of the sympathetic nervous system (1). These tumors have notable heterogeneity in clinical behavior, ranging from spontaneous regression or differentiation into a benign ganglioneuroma to rapid progression and death due to disease. A number of somatically acquired genetic abnormalities significantly influence the clinical outcome of these tumors. One of the most important genetic markers of unfavorable prognosis in these tumors is amplification of the *MYCN* transcription factor (2, 3), which affects the expression levels of a large number of genes (4) and miRNAs (5–7). Genome-wide analyses of MYCN binding sites indicate that MYCN binds to a few thousand sites throughout the genome, playing a role as both a transcription factor and a mediator of global chromatin structure (8–10).

Children with high-risk neuroblastoma are generally treated with intensive multi-modal chemotherapy, with 13-*cis*-retinoic acid included in the final part of the treatment regimen in an effort to eliminate minimal residual disease (11, 12). A related compound, all-*trans*-retinoic acid (ATRA) induces a number of neuroblastoma cell lines to undergo differentiation, with a significant increase in neurite length and a marked decrease in the rate of cell proliferation. SK-N-BE is a *MYCN*-amplified neuroblastoma cell line known to be responsive to ATRA (13). Transcriptional downregulation of *MYCN* precedes morphologic differentiation of neuroblastoma cells induced by ATRA, an event that is critical for both morphologic differentiation and for decreased cell proliferation (14, 15). Nitric oxide synthase (NOS1) is a signaling molecule that is upregulated following ATRA-induced differentiation of SK-N-BE cells which greatly accelerates the differentiation process when ectopically overexpressed (16). The mechanism leading to transcriptional upregulation of *NOS1* following ATRA-induced differentiation, however, is unknown. In a genome-wide analysis of DNA methylation patterns of SK-N-BE cells before and after ATRA-induced differentiation, we now show that DNA methylation alterations (predominantly demethylation events) affect many gene promoter regions following differentiation, including the *NOS1*

Authors' Affiliations: [1]Departments of Cancer Genetics, Royal College of Surgeons in Ireland, York House and [2]Children's Research Centre, Our Lady's Children's Hospital, Crumlin, Dublin, Ireland

Note: S. Das and N. Foley, co-first authors. P.G. Buckley and R.L. Stallings, co-senior authors.

Corresponding Author: Raymond L. Stallings, Royal College of Surgeons in Ireland, York House, York Street, Dublin, Ireland. Phone: 353-1402-8533; E-mail: rstallings@rcsi.ie.

doi: 10.1158/0008-5472.CAN-10-1534

gene. We also propose a novel model accounting for the widespread DNA methylation changes incurred during the differentiation of neuroblastoma cells involving the targeting of DNA methyltransferases by MYCN repressed miRNAs.

Materials and Methods

Cell culture and treatments

SK-N-BE, SH-SY5Y, SK-N-AS, and Kelly were obtained from the American Type Culture Collection whereas LAN-5 was obtained from the Children's Oncology Group Repository. Both repositories confirm cell line identities by genotyping and none of the lines were passaged in our laboratory for more than 6 months prior to use. Each line was also further validated by aCGH for previously published genomic imbalances. ATRA (5 pmol; Sigma) was continuously administered by replacing the medium every 24 hours for 7 days. Following fixation with paraformaldehyde, cell morphology was monitored using the neuronal specific antibody βIII tubulin (Abcam) followed by staining with an anti-rabbit Alexa 488–conjugated antibody (Invitrogen) as recommended by the suppliers. The MYCN repressible SHEP-TET21N cell line was obtained from Dr. Louis Chesler with the permission of Prof. Manfred Schwab and validated by aCGH. Cells were treated with 100 ng/mL of doxycycline to repress *MYCN* transcription. RNA was isolated after 48 hours. Kelly neuroblastoma cells were cultured in 10 mL of RPMI 1640 containing 5-aza-2′-deoxycytidine (Sigma-Aldrich) at a final concentration of 2 μg/mL for 72 hours.

Methylated DNA immunoprecipitation

The protocol used for methylated DNA immunoprecipitation (MeDIP) to microarrays analysis was as previously described by Murphy and colleagues (9). Four micrograms of sonicated DNA was incubated overnight with 10 μg of anti-5′ methyl-cytidine antibody (Eurogentec). MeDIP and input DNA were differentially labeled and hybridized to a CpG island promoter plus array from Roche NimbleGen as recommended by the manufacturer. Analysis was performed using the methylation application in NimbleScan version 2.4. Only peaks detected in duplicate experiments were used for further analysis. Methylation peaks mapping –2,000/+500 bp around the transcriptional start sites were used for further analysis. Raw log 2 ratio data for array experiments is available at http://www.ebi.ac.uk/arrayexpress (Accession E-TABM-964).

Microarray gene expression profiling

Total RNA was extracted from SK-N-BE cells using the Qiagen RNeasy Mini Kit and the SuperScript Double-Stranded cDNA Synthesis Kit (Invitrogen) was used to generate cDNA according to the protocols of the manufacturer. Cy3 labeling of ds-cDNA was performed overnight using the NimbleGen One-Color DNA Labeling Kit.

Four micrograms of Cy3-labeled ds-cDNA was hybridized to the *Homo sapiens* 4 × 72K gene expression array (Roche NimbleGen) representing 24,000 protein-coding genes, according to the protocols of the manufacturer. The mRNA expression data was analyzed using NimbleScan software version 2.4, which applied quantile normalization (17), and expression values were obtained using the Robust Multi-Chip Average algorithm as described by Irizarry and colleagues (18). Expressional alterations of 2-fold across both biological repeats were considered significant. Microarray expression data is available at http://www.ebi.ac.uk/arrayexpress (ArrayExpress Accession: E-MEXP-2557).

Bisulfite sequencing

A total of 500 ng of DNA from biological replicates for ATRA-treated and untreated cells was bisulfite-converted using the EZ DNA-methylation Gold Kit (Zymo). PCR primers were designed using methyl primer express (http://www.appliedbiosystems.com/methylprimerexpress). PCR products were purified using the QIAquick PCR purification kit (Qiagen) and sequenced at MWG Biotech. Methylated HeLa genomic DNA (New England Biolabs) was used as a positive control. Resulting electropherograms were analyzed using the BIQ analyzer (19).

Computational analysis

Compilation, smoothing, and preprocessing of data was carried out using in-house developed Java (v1.6) software. Prior to genomic correlation analysis of methylation profiles, mean smoothing was carried out over a 10-probe window and over gaps less than 100 bp. Analysis and visualization of genomic methylation was carried out using R statistical programming language (v2.10).

MicroRNA transfections

The Pre-miR to miR-152, and Pre-miR negative control 1 (Applied Biosystems) were introduced into the cells by reverse transfection using the transfection agent siPORT *Neo*FX (Ambion). Pre-mIR (30 nmol/L) was used in each transfection. Total RNA/miRNA was extracted 24, 48, and 72 hours after transfection using mirNeasy kit (Qiagen).

Reverse transcription and real-time PCR

Reverse transcription was carried out using 50 ng of total RNA and the High-Capacity Reverse Transcription Kit (Applied Biosystems). The following TaqMan assays were obtained from Applied Biosystems: *DNMT1*, Hs00945899_m1; *DNMT3A*, Hs00173377_m1; *DNMT3B*, Hs001171875_m1; miR-152, HS000475; and *NOS1*, Hs00167223_m1). qPCR analysis was performed in triplicate on the 7900 HT Fast Real-time System and glyceraldehyde-3-phosphate dehydrogenase was used for normalization in gene expression studies and RNU66 in microRNA assays. miRNA TaqMan Low Density Arrays (368TaqMan PCR assays; Applied Biosystems) were used for miRNA profiling, as described (5). A relative fold change in expression of the target gene transcript was determined using the comparative cycle threshold method ($2^{-\Delta\Delta CT}$).

Luciferase reporter

A 321-nt-long region (Fig. S1A) of the 3′ untranslated region (3′-UTR) of *DNMT1* containing the predicted miR-152 binding site was ligated into the psiCHECK-2 luciferase vector (Promega) 3′ of the luciferase gene. As a negative control, three

mutations were introduced into the seed region of the miR-152 binding site of this sequence (Fig. S1B). After 24 hours, the cells were cotransfected with either the pre–miR-152 mimic and luciferase construct or a scrambled negative control sequence and luciferase construct using LipofectAMINE 2000. Seventy-two hours after cotransfection, cells were lysed and luciferase activity was measured by Dual-Glo Luciferase Assay (Promega). All experiments were normalized to an internal firefly luciferase.

Western blot

Protein concentration was measured using the bicinchoninic acid assay from Pierce. Proteins were fractionized on 6% polyacrylamide gels, and blotted onto nitrocellulose membrane. The membrane was probed with the 1:1,000 anti-DNMT1 Antibody (Sigma), 1:500 anti-MYCN (NCM-II-100, Abcam), and anti-glyceraldehyde-3-phosphate dehydrogenase (Abcam). Signal was detected using Immobilon Western (Millipore).

Cell invasion assays

Invasion Assays were carried out using BD Biocoat Growth Factor–Reduced MATRIGEL Invasion Chambers (BD Biosciences) as recommended by the supplier.

Growth curve

Cells were set up in six-well plates at equal densities for transfections with miR-152 mimics, scrambled oligonucleotide negative control, and nontransfected cells. Cells were harvested from six-well plates at 24-, 48-, 72-, and 96-hour time points and hemocytometer counts were averaged from triplicate wells.

Acid phosphatase assay for cell proliferation

Cells were transfected in 96-well plates (10^3 cells per well). At 96 hours, wells were washed twice with PBS and 10 mmol/L of *p*-nitrophenol phosphate in 0.1 mol/L of sodium acetate with 0.1% triton X-100 was added. Plates were incubated at 37°C for 2 hours when the reaction was stopped with 50 μL of 1 mol/L sodium hydroxide per well. Absorbance was measured at 405 nm. Values were normalized to the scrambled oligonucleotide negative control.

Colony-forming efficiency

A 1% agarose solution was plated on 10 cm^2 Petri dishes and cells were plated at 1.5×10^6 in 10 mL of culture medium. Colonies were stained with 0.1% crystal violet, photographed, and counted in replicate studies.

Results

Identification of recurrent DNA methylation changes at CpG islands and promoter regions following ATRA treatment

ATRA treatment induced SK-N-BE cells to undergo differentiation, as evidenced by the outgrowth of neurites (Fig. 1A), a decrease in cell growth (Fig. S2A), and a substantial decrease in *MYCN* mRNA and protein (Fig. S2B and C). To assess a potential role for DNA methylation alterations in the process of ATRA-induced neuroblastoma cell differentiation, anti–methyl-cytidine immunoprecipitated DNA and non-immunoprecipitated input DNAs from untreated and ATRA-treated SK-N-BE were hybridized to microarrays containing 33,485 tiled regions representing all known promoter and CpG island regions. In total, 2,499 and 1,721 promoter and nonpromoter CpG island sites were hypermethylated in untreated and treated SK-N-BE cells, respectively. A pairwise comparison of log 2 ratio values from MeDIP biological replicates resulted in a Pearson correlation coefficient of 0.87 for the ATRA-treated SK-N-BE cells and 0.93 for untreated cells, indicating highly significant reproducibility of experimental results (Fig. S3A and B). In contrast, comparison of ATRA-treated versus untreated cells yielded a lower correlation coefficient of 0.80, indicating that epigenetic changes have occurred in ATRA-treated cells (Fig. S3C).

In total, 402 gene promoters (excluding nonpromoter CpG island sites) were demethylated following ATRA treatment (across two biological replicates), with 82 of these genes being overexpressed greater than 2-fold in the ATRA-treated cells (7 d post-ATRA) relative to untreated, as ascertained by mRNA expression microarrays (Fig. 1B; Table S1). In contrast, only 88 genes became hypermethylated following ATRA treatment, 13 of which were underexpressed in ATRA-treated cells by >2-fold (Fig. 1B; Table S1). The demethylation of promoter regions in ATRA-treated and untreated cells was confirmed following sequencing of bisulfite-converted DNA from representative genomic regions (Table S2).

Gene ontology analysis of the genes that were demethylated and re-expressed after ATRA treatment indicated that signal transduction was the only significantly enriched category ($P = 0.0069$; Table S1). One of these demethylated signal transduction genes, *NOS1* (Fig. 1C; Table S2), was re-expressed 10.6-fold ($P = 0.0009$) at 48 hours post-ATRA and persisted at >20-fold between 6 and 9 days post-ATRA (validated by qPCR; Fig. 1D). This gene was of particular interest because it has been shown to promote neuroblastoma cell differentiation (16), indicating that some of the demethylated and re-expressed genes are functionally relevant for the process of differentiation.

To determine if the demethylation and re-expression of *NOS1* is a general phenomenon occurring during ATRA-induced neuroblastoma cell differentiation, we treated two additional sensitive cell lines (SH-SY5Y and LAN-5) with ATRA, along with an insensitive cell line, SK-N-AS, as a negative control. ATRA caused a pronounced outgrowth of neurites in SH-SY5Y and LAN-5, but not in SK-N-AS (Fig. S4A-F), and *MYCN* transcript levels were significantly reduced in SH-SY5Y and LAN-5 (Fig. S2D). Sequencing of bisulfite-converted DNA indicated substantial demethylation of the *NOS1* promoter region (Fig. S5A), which resulted in significant *NOS1* re-expression (Fig. S5B) following ATRA treatment of SH-SY5Y and LAN-5. SK-N-AS, on the other hand, showed a slight increase in methylation and no re-expression was detectable. To further confirm that demethylation was responsible for *NOS1* overexpression, we treated an independent

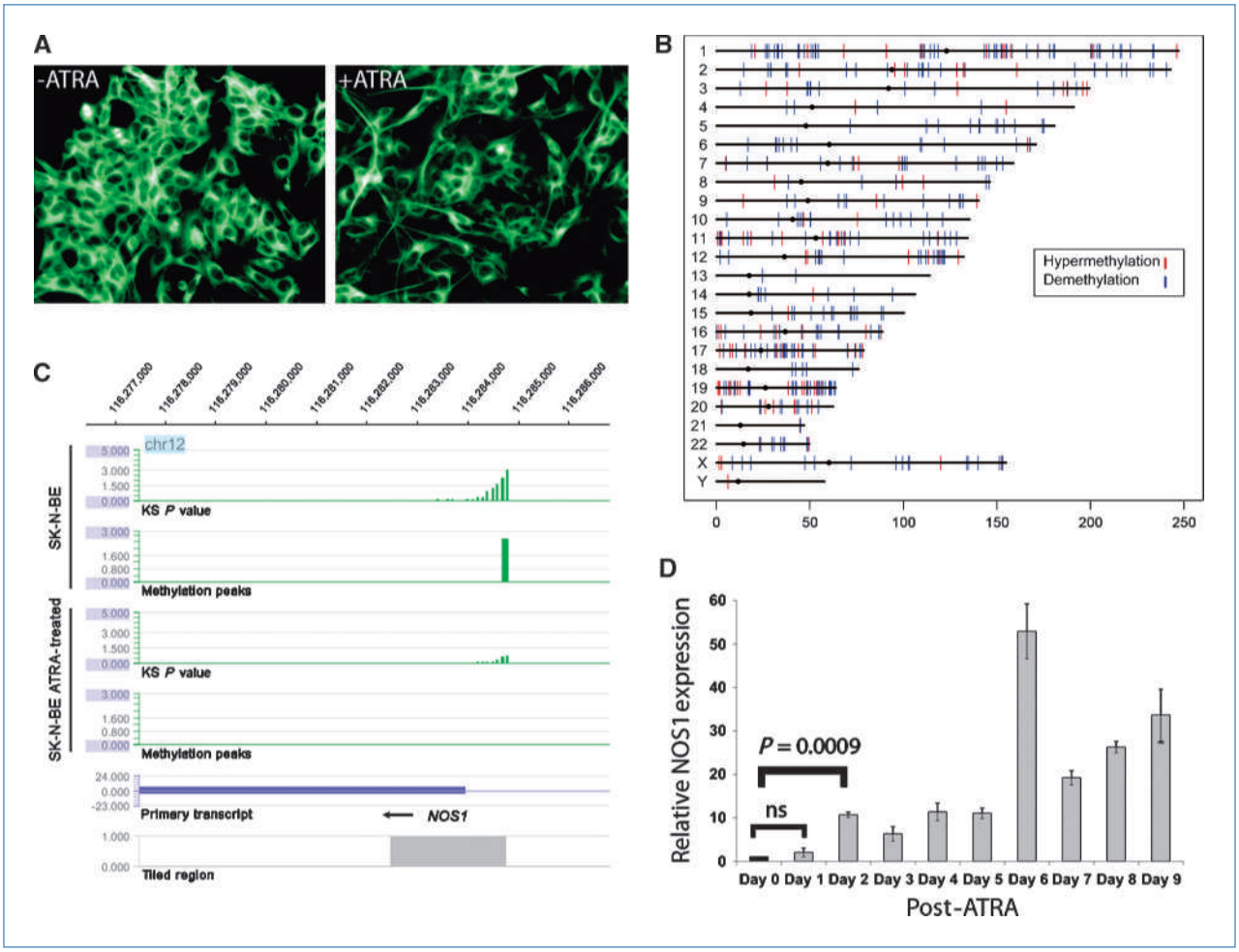

Figure 1. ATRA treatment of the neuroblastoma cell line SK-N-BE and its effect on DNA methylation and *NOS1* expression. A, SK-N-BE cells pre- and 7 d post-ATRA treatment are displayed. Cells were stained using an antibody for the neuronal marker βIII tubulin. B, graphical display of the sites which became demethylated (vertical blue lines; $n = 402$) or hypermethylated (vertical red lines; $n = 82$) on each chromosome in SK-N-BE cells following 7 d of ATRA treatment. Centromere positions are depicted by circles and the horizontal axis represents genome position in megabases. C, graphical display of MeDIP-chip results for *NOS1* promoter. A hypermethylated region upstream of the *NOS1* locus in the SK-N-BE cell line is indicated by statistically significant *P* values derived from a one-sided Kolmogorov-Smirnov test (KS) which are binned as a methylated peak (bottom). Upon ATRA treatment, the level of methylated DNA enrichment is significantly diminished as indicated by the reduced KS scores. The position and orientation of the *NOS1* gene is indicated by the blue bar. The gray bar denotes the tiled region analyzed on the array around the *NOS1* promoter region. D, *NOS1* qPCR expression analysis of SK-N-BE cells from days 1 to 9 post-ATRA (all time points are relative to day 0, untreated). A statistically significant increase in *NOS1* levels is detected at day 2 post-ATRA.

neuroblastoma cell line, Kelly, with the demethylating agent 5-aza-deoxycytidine, which resulted in a 10-fold increase in *NOS1* expression following 3 days of 5-aza-deoxycytidine exposure (Fig. S6). We conclude that functionally significant demethylation of the *NOS1* promoter sequence is a general occurrence during ATRA-induced differentiation of neuroblastoma cells.

Molecular mechanisms leading to genome-wide demethylation events in ATRA-treated cells

Diminished expression of DNA methyltransferase *DNMT1* is known to cause genome-wide demethylation events (20), and our mRNA expression microarray analyses indicated that *DNMT1*, as well as *DNMT3B*, were significantly downregulated following ATRA treatment of SK-N-BE cells. qPCR analysis confirmed a statistically significant decrease in gene expression for *DNMT1* and *DNMT3B* in SK-N-BE, as well as in SH-SY5Y and LAN-5 following ATRA treatment (Fig. 2A). Conversely, ATRA-insensitive SK-N-AS cells displayed a modest, but statistically significant, increase in *DNMT1* and *DNMT3B* transcripts (Fig. 2A), which might explain the overall increase in methylation detected at the *NOS1* promoter following ATRA treatment (Fig. S5A). We conclude that DNMT downregulation is a general feature of ATRA-sensitive neuroblastoma cell lines, but not for lines that are insensitive to ATRA treatment.

None of the *DNMT* genes displayed promoter region methylation before or after ATRA treatment (MeDIP analysis), indicating that methylation was not responsible for their

downregulation following ATRA exposure. To determine if upregulated miRNAs might be causally related to *DNMT* downregulation following ATRA treatment of SK-N-BE, we carried out expression analysis for 368 miRNAs using low-density TaqMan arrays. Seventeen miRNAs were overexpressed by at least 2-fold in two biological replicates of ATRA-treated SK-N-BE cells, and 17 miRNAs had a 2-fold or greater decrease in expression (Fig. S7). MiR-152, which has an 8-mer conserved seed match with *DNMT1*, increased 2.5-fold following ATRA treatment, which was validated using an individual qPCR assay following ATRA treatment of SK-N-BE, SH-SY5Y, and LAN-5 (Fig. 2B). Thus, overexpression of miR-152 in response to ATRA might account for the reduction of *DNMT1*. This was validated by transfection of mature miR-152 mimics into SK-N-BE cells (Fig. S8), which resulted in the downregulation of *DNMT1* on mRNA expression microarrays. This was validated by qPCR and at the protein level by Western blot (Fig. 2C), indicating that endogenous upregulation of miR-152 in ATRA-treated cells is the likely cause for DNMT1 reduction. In addition, cotransfection of a luciferase reporter construct containing a segment of the *DNMT1* 3′-UTR inclusive of the miR-152 target site with mature miR-152 mimics into SK-N-BE led to a significant reduction in luciferase activity relative to cotransfection with a scrambled negative control (Fig. 2D). Mutation of the miR-152 target site abrogated the reduction in luciferase activity, leading us to conclude that miR-152 directly targets *DNMT1*, consistent with a report by Branconi and colleagues demonstrating miR-152 targeting of *DNMT1* in a gallbladder cancer cell line (21).

Expression microarray analysis also indicated that ectopic upregulation of miR-152 had a global effect on the transcriptome of SK-N-BE cells, leading to the downregulation of 3,483 genes and the upregulation of 2,765 genes. For genes downregulated by >3.0-fold, there was a statistically significant (P = 0.01) enrichment of conserved miR-152 target sites in their 3′-UTR region, whereas upregulated genes (>1.5-fold) had a statistically significant (P = 0.01) decrease in miR-152 target sites (Fig. 3). These results indicate that miR-152 overexpression has both direct and indirect effects on the transcript levels of large numbers of genes.

The mechanism leading to increased miR-152 levels following ATRA treatment could be related to diminished *MYCN* expression, which occurs within 6 hours after ATRA exposure (ref. 15; also Fig. S2B). We have previously shown that miR-152 is expressed at significantly lower levels in *MYCN*-amplified primary tumors relative to those lacking it (5), indicating that MYCN either directly or indirectly represses this miRNA. To further validate the repression of miR-152 by MYCN in an experimental system, we evaluated

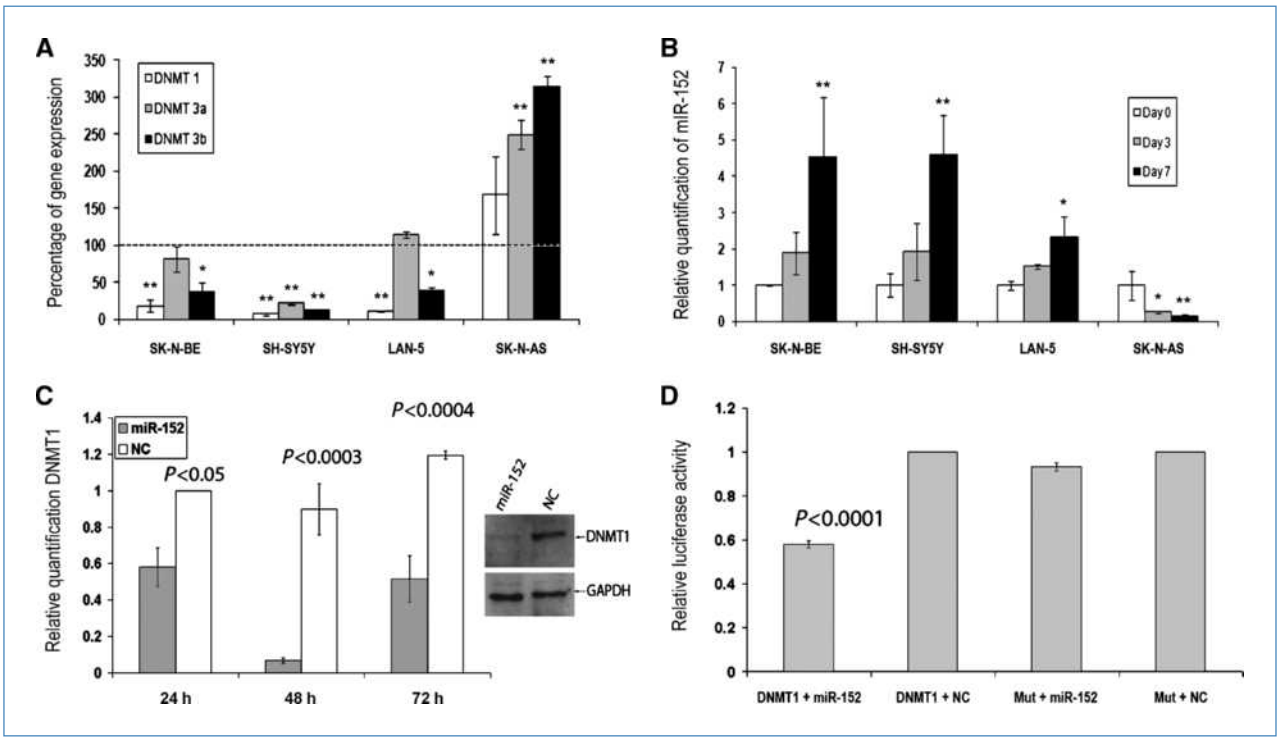

Figure 2. ATRA-induced differential expression of DNMTs and miR-152. A, expression values ascertained by TaqMan qPCR for *DNMT1, DNMT3A,* and *DNMT3B* pre- and post-ATRA treatment of SK-N-BE, SH-SY5Y, LAN-5, and SK-N-AS are plotted. Graph shows percentage of change in *DNMT* expression in ATRA-treated cells relative to untreated. B, expression levels of miR-152 in ATRA-treated SK-N-BE, SH-SY5Y, LAN-5, and SK-N-AS cells (*, $P < 0.05$ and **, $P < 0.01$, values relative to untreated cells). C, negative effect of ectopic overexpression of miR-152 in SK-N-BE cells on *DNMT1* mRNA and protein levels. NC is a negative control transfected with a scrambled oligonucleotide sequence. D, cotransfection of a luciferase reporter construct containing a 321-bp segment of *DNMT1* 3′-UTR inclusive of the miR-152 target site with miR-152 mature mimics into Kelly cells.

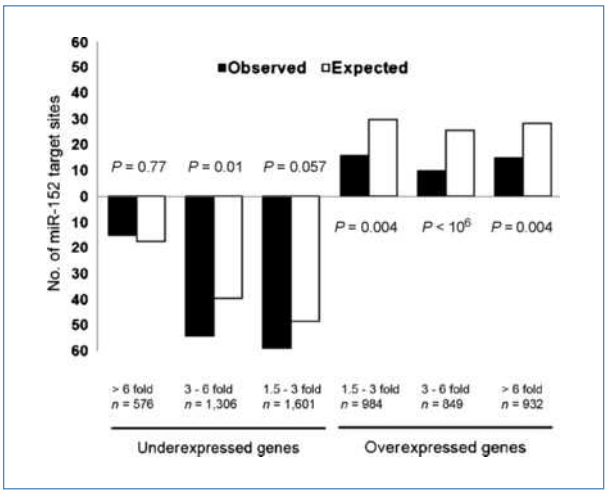

Figure 3. Analysis of conserved miR-152 predicted target sites in 3′-UTR regions of mRNAs that are underexpressed (left) or overexpressed (right) following miR-152 ectopic upregulation. Black columns are the observed number of genes with predicted target sites whereas the white columns represent the number of expected target sites based on the analysis of 10^6 randomly generated miRNA–mRNA interactions. Genes that are underexpressed 3-fold to 6-fold show a statistically significant enrichment of miR-152 target sites, whereas there is a statistically significant inverse correlation between miR-152 predicted 3′-UTR target sites and genes that are overexpressed.

the effects of changing MYCN levels in the SHEP-TET21N cell line (22), which contains a doxycycline repressible *MYCN* construct, on miR-152 levels. MiR-152 expression increased ~3-fold within 48 hours after *MYCN* depletion (Fig. 4), whereas *DNMT1* mRNA levels decreased by ~5-fold, experimentally confirming an inverse relationship between *MYCN* and miR-152 expression. The mechanism leading to decreased *DNMT3B* mRNA levels following ATRA is uncertain, although this too could be miRNA-driven. MiR-125a/b and miR-26a/b, predicted to target *DNMT3B*, are upregulated in ATRA-treated cells (ref. 23; ~1.5-fold upregulation in our experiments). Our model for the molecular events leading to ATRA-induced differentiation is illustrated in Fig. 5.

Biological effects of miR-152 ectopic overexpression in SK-N-BE cells

A number of studies have shown that ectopic overexpression of some miRNAs, the endogenous levels of which are increased in response to ATRA, have phenotypic effects that correspond to an ATRA-induced phenotype (23–25). Ectopic upregulation of miR-152 in SK-N-BE cells resulted in a significant decline in cell invasiveness and anchorage-independent cell growth, but had no effect on the rate of accumulation of cell numbers (Fig. S9 A–D). It also did not cause the outgrowth of lengthy neurites similar to those observed following ATRA treatment. Although upregulation of miR-152 by itself cannot fully account for ATRA-induced differentiation, it does have significant biological effects that contribute towards this phenotype.

Discussion

This study represents the first genome-wide analysis of DNA methylation changes in neuroblastoma cells induced to undergo differentiation by ATRA, revealing the extensive nature of epigenomic changes. On a gene-specific basis, others have also reported DNA methylation changes in other cell types treated with ATRA. For example, Love and colleagues (26) showed that ATRA treatment of HL60 leukemia cells leads to hypermethylation of the *TERT* promoter, possibly caused by aberrant expression of DNA methyltransferases. Rowling and colleagues (27), on the other hand, reported that rats treated with ATRA exhibited an overall decrease in endogenous levels of DNA methylation, consistent with our *in vitro* study indicating an overall reduction of methylation at gene promoters (27). Although DNMT levels were not assessed in the report by Rowling and colleagues (27), the authors propose an alternative mechanism in which levels of glycine *N*-methyltransferase are increased in response to ATRA treatment, leading to a reduction in levels of *S*-adenosyl-methionine, which acts as a substrate in numerous transmethylation reactions and its limited availability might be responsible for the observed reduction in methylation levels. In contrast, Nouzova and colleagues (28), using different assessment methods and a significantly lower resolution microarray platform than what was applied in our study, did not observe changes in DNA methylation, but did report increases of histone acetylation at 282 CpG islands and decreases at 34 loci. Their observation of overall increased histone acetylation following ATRA, however, is consistent with our observation of overall decreased DNA

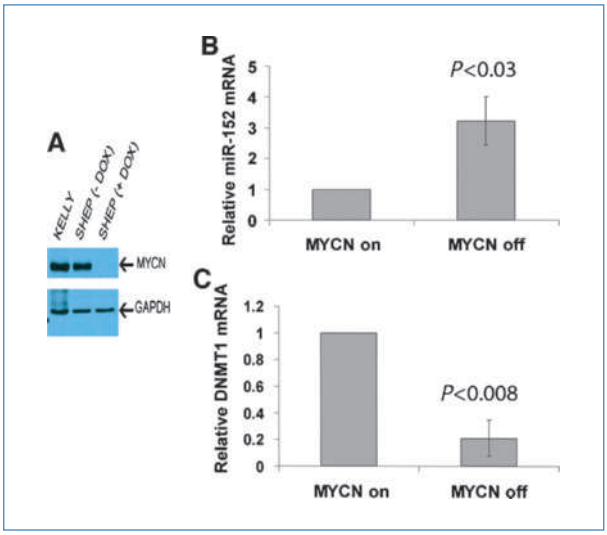

Figure 4. Experimental validation of an inverse relationship between MYCN and miR-152 levels using the SHEP-TET21 cell line containing a doxycycline (DOX) repressible *MYCN* transgene. A, Western blot showing reduction in MYCN protein following the addition of doxycycline to the cell culture medium. B, miR-152 levels increase in MYCN depleted cells (48 h post-doxycycline). C, *DNMT1* mRNA levels are decreased 5-fold (48 h post-doxycycline).

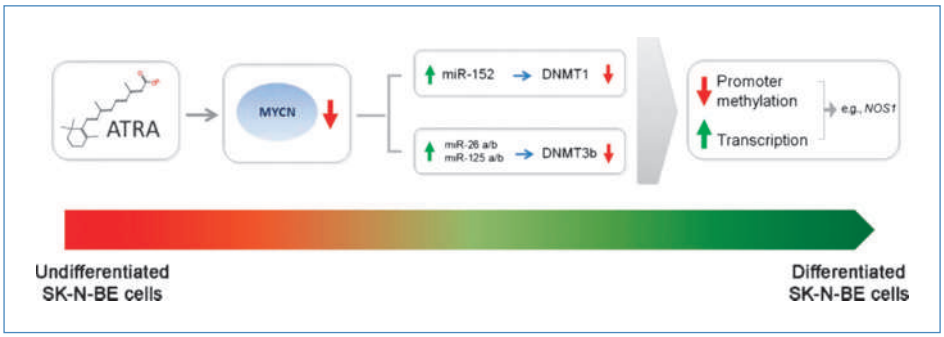

Figure 5. Model illustrating regulatory changes during differentiation of SK-N-BE cells induced by ATRA. ATRA treatment causes downregulation of MYCN, leading to overexpression of MYCN repressed miRNAs miR-152, miR-26a/b, and miR-125a/b, which downregulate the DNA methyltransferases *DNMT1* (experimentally validated) and *DNMT3B* (computationally predicted) targets, respectively. The downregulation of DNA methyltransferases, in turn, leads to the demethylation and upregulation of numerous genes such as *NOS1*, which promote neural cell differentiation.

methylation in that both are associated with a transcriptionally active chromatin state.

The downregulation of *DNMTs* after ATRA is a potential explanation for the observed overall decrease in DNA methylation in the differentiated cells. In addition, the upregulation of miRNAs that target these *DNMT*s is the most plausible explanation for their reduction following ATRA treatment. Moreover, miRNAs targeting DNMTs, such as miR-152 and miR-26a/b, seem to be either directly or indirectly repressed by MYCN, given that they are underexpressed in MYCN-amplified primary tumors (5, 7). Thus, the downregulation of MYCN in ATRA-treated SK-N-BE cells accounts for the upregulation of these *DNMT* targeting miRNAs.

Ciani and colleagues (16) suggested that *NOS1* upregulation in response to ATRA is responsible for the downregulation of *MYCN* transcription. They proposed that NOS1 causes dephosphorylation of RB, which then leads to the sequestration of E2F transcription factors, which positively regulate MYCN, in an RB-E2F protein complex. In this model, the depletion of E2Fs results in the transcriptional downregulation of *MYCN*. The timing of events following ATRA treatment, however, is inconsistent with this model. As shown by Thiele and colleagues (15), *MYCN* transcriptional downregulation is detectable within 6 hours after ATRA exposure whereas Ciani and colleagues (16) showed that endogenous NOS1 protein is only detectable between days 5 and 7 after ATRA. Here, we further show that *NOS1* mRNA increase is not detectable until 48 hours post-ATRA. The timing of these events is more consistent with our model (Fig. 5), whereby early *MYCN* downregulation leads to the upregulation of miRNAs that target *DNMT*s. The late appearance of *NOS1* expression is then the consequence of demethylation of the *NOS1* gene promoter sequence followed by transcriptional activation. The molecular mechanism leading to *MYCN* downregulation remains unknown, although a number of miRNAs predicted to target *MYCN* are upregulated following ATRA treatment (e.g., miR-24, miR-214, and let-7e).

MiR-128, also upregulated in response to ATRA, inhibits neuroblastoma cell motility and invasiveness through direct targeting of the Reelin and DCX genes (24). Here, we show that ectopic upregulation of miR-152, which also becomes endogenously overexpressed following ATRA exposure, negatively regulates cell invasiveness and anchorage-independent cell growth, but does not induce differentiation or inhibit cell growth. The genes being targeted by miR-152 that negatively affect cell invasiveness and anchorage-independent cell growth remain to be elucidated. The signaling pathways activated following the exposure of neuroblastoma cells to ATRA are complex and include the activation of additional miRNAs that affect cell proliferation and neurite outgrowth. The neuronal-specific miRNAs-9, 125a, and 125b are upregulated in response to ATRA and target neurotrophin receptor tropomyosin-related kinase C, a protein that is critical for regulating neuroblastoma cell growth (23). Moreover, ectopic upregulation of miR-125b was also determined to promote neuronal differentiation of the neuroblastoma SH-SY5Y cell line through antagonizing a number of neuronal genes (25).

In conclusion, the DNA methylation changes observed on ATRA treatment further illustrate the dynamic nature of the epigenome. At least one of the genes that becomes demethylated and expressed in response to ATRA, *NOS1*, is clearly implicated in neuroblastoma cell differentiation (16), indicating that epigenetic changes play important functional roles in this process. Whether DNA methylation changes affecting the expression of other gene sequences or miRNAs have functional relevance for differentiation is an interesting question warranting further study.

Disclosure of Potential Conflicts of Interest

No potential conflicts of interest were disclosed.

Grant Support

Science Foundation Ireland (07/IN.1/B1776), Children's Medical and Research Foundation, Cancer Research Ireland, and the NIH (5R01CA127496). P.G. Buckley is supported by a post-doctoral fellowship from IRCSET.

The costs of publication of this article were defrayed in part by the payment of page charges. This article must therefore be hereby marked *advertisement* in accordance with 18 U.S.C. Section 1734 solely to indicate this fact.

Received 04/29/2010; revised 08/18/2010; accepted 08/18/2010; published OnlineFirst 09/14/2010.

References

1. Brodeur GM. Neuroblastoma: biological insights into a clinical enigma. Nat Rev Cancer 2003;3:203–16.
2. Seeger RC, Brodeur GM, Sather H, et al. Association of multiple copies of the N-myc oncogene with rapid progression of neuroblastomas. N Engl J Med 1985;313:1111–6.
3. Brodeur GM, Seeger RC, Schwab M, Varmus HE, Bishop JM. Amplification of N-myc in untreated human neuroblastomas correlates with advanced disease stage. Science 1984;224:1121–4.
4. Alaminos M, Mora J, Cheung NK, et al. Genome-wide analysis of gene expression associated with MYCN in human neuroblastoma. Cancer Res 2003;63:4538–46.
5. Bray I, Bryan K, Prenter S, et al. Widespread dysregulation of MiRNAs by MYCN amplification and chromosomal imbalances in neuroblastoma: association of miRNA expression with survival. PLoS One 2009;4:e7850.
6. Chen Y, Stallings RL. Differential patterns of microRNA expression in neuroblastoma are correlated with prognosis, differentiation, and apoptosis. Cancer Res 2007;67:976–83.
7. Mestdagh P, Fredlund E, Pattyn F, et al. MYCN/c-MYC-induced microRNAs repress coding gene networks associated with poor outcome in MYCN/c-MYC-activated tumors. Oncogene;29:1394–404.
8. Cotterman R, Jin VX, Krig SR, et al. N-Myc regulates a widespread euchromatic program in the human genome partially independent of its role as a classical transcription factor. Cancer Res 2008;68:9654–62.
9. Murphy DM, Buckley PG, Bryan K, et al. Global MYCN transcription factor binding analysis in neuroblastoma reveals association with distinct E-box motifs and regions of DNA hypermethylation. PLoS One 2009;4:e8154.
10. Westermann F, Muth D, Benner A, et al. Distinct transcriptional MYCN/c-MYC activities are associated with spontaneous regression or malignant progression in neuroblastomas. Genome Biol 2008;9:R150.
11. Pahlman S, Ruusala AI, Abrahamsson L, Mattsson ME, Esscher T. Retinoic acid-induced differentiation of cultured human neuroblastoma cells: a comparison with phorbolester-induced differentiation. Cell Differ 1984;14:135–44.
12. Wagner LM, Danks MK. New therapeutic targets for the treatment of high-risk neuroblastoma. J Cell Biochem 2009;107:46–57.
13. Melino G, Thiele CJ, Knight RA, Piacentini M. Retinoids and the control of growth/death decisions in human neuroblastoma cell lines. J Neurooncol 1997;31:65–83.
14. Thiele CJ, Israel MA. Regulation of N-myc expression is a critical event controlling the ability of human neuroblasts to differentiate. Exp Cell Biol 1988;56:321–33.
15. Thiele CJ, Reynolds CP, Israel MA. Decreased expression of N-myc precedes retinoic acid-induced morphological differentiation of human neuroblastoma. Nature 1985;313:404–6.
16. Ciani E, Severi S, Contestabile A, Bartesaghi R. Nitric oxide negatively regulates proliferation and promotes neuronal differentiation through N-Myc downregulation. J Cell Sci 2004;117:4727–37.
17. Bolstad BM, Irizarry RA, Astrand M, Speed TP. A comparison of normalization methods for high density oligonucleotide array data based on variance and bias. Bioinformatics 2003;19:185–93.
18. Irizarry RA, Hobbs B, Collin F, et al. Exploration, normalization, and summaries of high density oligonucleotide array probe level data. Biostatistics 2003;4:249–64.
19. Bock C, Reither S, Mikeska T, Paulsen M, Walter J, Lengauer T. BiQ Analyzer: visualization and quality control for DNA methylation data from bisulfite sequencing. Bioinformatics 2005;21:4067–8.
20. Robert MF, Morin S, Beaulieu N, et al. DNMT1 is required to maintain CpG methylation and aberrant gene silencing in human cancer cells. Nat Genet 2003;33:61–5.
21. Braconi C, Huang N, Patel T. MicroRNA-dependent regulation of DNA methyltransferase-1 and tumor suppressor gene expression by interleukin-6 in human malignant cholangiocytes. Hepatology 2009;51:881–90.
22. Lutz W, Stohr M, Schurmann J, Wenzel A, Lohr A, Schwab M. Conditional expression of N-myc in human neuroblastoma cells increases expression of α-prothymosin and ornithine decarboxylase and accelerates progression into S-phase early after mitogenic stimulation of quiescent cells. Oncogene 1996;13:803–12.
23. Laneve P, Di Marcotullio L, Gioia U, et al. The interplay between microRNAs and the neurotrophin receptor tropomyosin-related kinase C controls proliferation of human neuroblastoma cells. Proc Natl Acad Sci U S A 2007;104:7957–62.
24. Evangelisti C, Florian MC, Massimi I, et al. MiR-128 up-regulation inhibits Reelin and DCX expression and reduces neuroblastoma cell motility and invasiveness. FASEB J 2009;23:4276–87.
25. Le MT, Xie H, Zhou B, et al. MicroRNA-125b promotes neuronal differentiation in human cells by repressing multiple targets. Mol Cell Biol 2009;29:5290–305.
26. Love WK, Berletch JB, Andrews LG, Tollefsbol TO. Epigenetic regulation of telomerase in retinoid-induced differentiation of human leukemia cells. Int J Oncol 2008;32:625–31.
27. Rowling MJ, McMullen MH, Schalinske KL. Vitamin A and its derivatives induce hepatic glycine N-methyltransferase and hypomethylation of DNA in rats. J Nutr 2002;132:365–9.
28. Nouzova M, Holtan N, Oshiro MM, et al. Epigenomic changes during leukemia cell differentiation: analysis of histone acetylation and cytosine methylation using CpG island microarrays. J Pharmacol Exp Ther 2004;311:968–81.